JOURNAL OF GEOPHYSICAL RESEARCH, VOL. 103, NO. D22, PAGES 28,701–28,710, NOVEMBER 27, 1998

Accuracy of absolute precipitable water vapor estimates from GPS observations

Paul Tregoning

Research School of Earth Sciences, The Australian National University, Canberra

Reinout Boers and Denis O'Brien

CSIRO Atmospheric Research, Aspendale, Australia

Martin Hendy

Australian Surveying and Land Information Group, Canberra

Abstract. We present GPS, radiosonde and microwave radiometer (MWR) estimates of precipitable water vapor (PW) at Cape Grim, Tasmania, during November and December 1995. The rms differences between GPS and radiosonde, MWR and radiosonde and GPS and MWR estimates of PW were 1.5 mm, 1.3 mm and 1.4 mm, respectively, whilst the biases between the three systems were ~0.2 mm. However, there are occasions when the amount of PW was under-estimated by GPS whilst at other times was over-estimated by MWR. The average overlap error of the GPS estimates of PW between adjacent daily solutions is related to the orbit overlap error and we removed a 2 mm bias introduced using International GPS Service orbits by estimating more accurate global orbits. The discrepancies of up to 3-4 mm between the MWR and GPS systems are not caused by rain, waveguide losses, varying waveguide temperature, detector non-linearity or inaccurate estimates of the mean radiating temperature of the atmosphere. However, small differences between mapping functions at low elevations can produce biases comparable with the bias between the two systems. Consequently, we suspect that the biases arise because the mapping functions do not represent the localized atmospheric conditions at Cape Grim. The most accurate GPS estimates are achieved when the GPS analysis contains station separations of more than 2000 km, an elevation cutoff angle of 12° is used and the CFA2.2 wet mapping function is used to map the wet delay at any angle to the delay in the zenith.

1. Introduction

Since the inception of space geodesy, the tropospheric delay of signals propagating through the atmosphere of the Earth has affected geodetic estimations of coordinates of points on the surface of the Earth. The amount of precipitable water vapor (PW) contained in the neutral atmosphere can be inferred from the propagation delay of Global Positioning System (GPS) signals passing through the troposphere. For many years, geodesists have treated such delays as nuisance parameters to be removed in the process of estimating station coordinates. Recent research has shown that the estimates of the wet tropospheric delay from very long baseline interferometry (VLBI) and GPS observations agree closely with estimates from radiosonde launches and microwave radiometer (MWR) measurements [e.g., *Duan et al.*, 1996]. Mathematical techniques have been developed to map the delay at any elevation to delay in the zenith (or vertical) direction, and the removal of the tropospheric delay by estimation has become an integral part of precise VLBI and GPS analyses [e.g., *Niell*, 1996; *Herring*, 1992; *MacMillan and Ma*, 1994].

The Global Positioning System consists of a constellation of satellites which transmit on two L-band frequencies (1575.42 MHz for $L1$ and 1227.6 MHz for $L2$) [*Spilker*, 1980]. These two signals are delayed as they propagate through the atmosphere due to the presence of atmospheric water vapor. This "wet delay" is detectable in geodetic analyses of GPS phase observations and can be transformed into an estimate of the PW present in the troposphere [e.g., *Bevis et al.*, 1992, 1994; *Rocken et al.*, 1993; *Duan et al.*, 1996]. Recent studies from small-scale networks (~50 km) [e.g., *Bevis et al.*, 1992, 1994; *Rocken et al.*, 1993] have demonstrated that PW can be estimated from GPS observations with an accuracy of better than 2 mm relative to a fixed GPS station. *Rocken et al.* [1995] showed that the relative estimates could be calibrated or "levered" to absolute values if there was an absolute estimate of PW (e.g., from a microwave radiometer) at one of the GPS stations. Long baselines reduce the high level of correlation of the tropospheric delays which occurs on short baselines [*Rocken et al.*, 1993; *Duan et al.*, 1996] and *Duan et al.* [1996] showed that absolute values of PW can be derived directly from GPS observations if GPS stations with separations greater than 500 km are included in the analysis; however, they do not

Paper number 98JD02516.
0148-0227/98/98JD-02516$09.00

quantify the minimum baseline length required in order to achieve this.

We studied the sensitivity of the accuracy of absolute estimates of PW derived from GPS observations by comparing the GPS and MWR estimates of PW at Cape Grim (northwestern Tasmania) (Figure 1) for a 6 week period in November and December 1995. For some of this period there were radiosonde launches at the GPS site as part of the first Aerosol Characterization Experiment (ACE1) [*Bates et al.*, 1997]. The microwave radiometer was calibrated against the radiosonde estimates of PW and the resulting retrieval coefficients were extrapolated across the periods without radiosonde launches in order to compare MWR and GPS estimates of PW. GPS data from sites in the International GPS Service (IGS) network [*Neilan*, 1997] were included in the analysis, and we varied the network configuration in order to determine the relationship between the network and the accuracy of absolute PW estimates.

The quality of results presented in this paper are equivalent to other results previously published on estimating PW from GPS, radiosondes and MWR [e.g., *Duan et al.*, 1996; *Rocken et al.*, 1995; *Emardson et al.*, 1998]. However, we show that there are still occasions where significant errors occur in one of the systems, resulting in discrepancies of up to 3-4 mm PW. Thus an average root mean square (rms) of 1.5 mm does not guarantee accuracy of that level at all times, and users should be careful about assuming that GPS can estimate accurate PW values at all times. Readers are referred to *Bevis et al.* [1992] and *Duan et al.* [1996] for a comprehensive discussion of the theory of GPS meteorology. Our analyses follow the procedure of *Duan et al.* [1996], and we use their nomenclature in this paper.

2. Modeling of Atmospheric Delay

The atmospheric delay of the GPS signals occurs in the ionosphere and the neutral atmosphere of the Earth. The ionospheric delay can be removed by utilizing its dispersive properties and the two frequencies of the GPS signals [*Gu and Brunner*, 1990]. The delay caused by the neutral atmosphere can be separated into two components: the zenith hydrostatic delay (ZHD) as a result of the induced dipole moment [*Duan et al.*, 1996] and a zenith wet delay (ZWD) due to the permanent dipole moment of PW and liquid water (LW) present in the troposphere [*Bevis et al.*, 1994]. Any errors in the modeled hydrostatic delay will be absorbed into the ZWD and will be transformed into an error in the PW estimates. To obtain an accuracy of 1 mm in the PW estimates, the surface pressure must be accurate to at least 0.3 hPa [*Elgered et al.*, 1991] so that the hydrostatic delay can be removed from the total zenith neutral delay (ZND) leaving only the delay due to the presence of PW in the neutral atmosphere. PW is the total quantity of water vapor above a point on the surface of the Earth expressed as the height of an equivalent column of liquid water [*Duan et al.*, 1996]. Typical atmospheric values are 25 mm for PW and 0.1 mm for LW, so the contribution of LW to total precipitable water is mostly smaller than 1%.

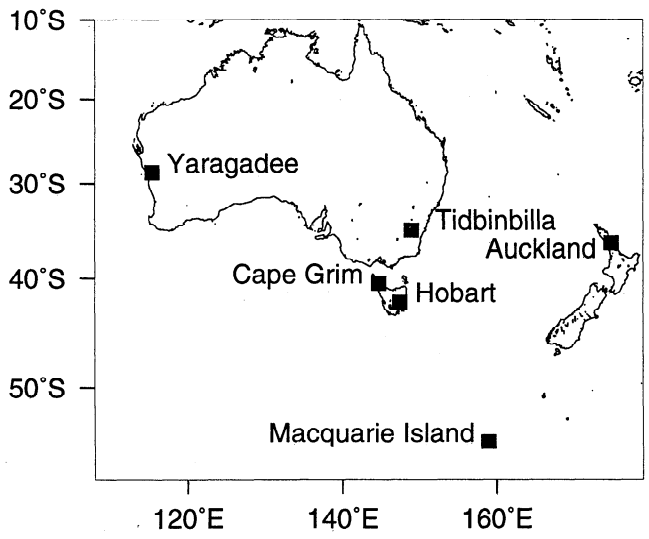

Figure 1. Location of Global Positioning System (GPS) sites used in the analyses of the GPS data.

The wet component of the ZND can be represented by

$$\mathrm{PW} = \Pi \times \mathrm{ZWD} \tag{1}$$

where

$$\Pi = \frac{10^6}{\rho R_v \left[(k_3 / T_m) + k_2' \right]} \tag{2}$$

[*Askne and Nordius*, 1987; *Bevis et al.*, 1994], where ρ is the density of liquid water, R_v is the specific gas constant for water vapor, k_3 and k_2' are physical constants [*Smith and Weintraub*, 1953], and T_m is the mean temperature of the atmosphere. T_m is defined [*Davis et al.*, 1985] as

$$T_m = \frac{\int (P_v / T) dz}{\int (P_v / T^2) dz} \tag{3}$$

where T is the temperature, and P_v is the partial pressure of water vapor. T_m can be inferred either from surface temperature measurements [*Bevis et al.*, 1992] or from numerical weather models [*Bevis et al.*, 1994; *Quinn and Herring*, 1996] with an accuracy of about 2%. Therefore the greatest possible error source in the conversion from ZWD to PW is likely to be the error in the initial geodetic estimate of the ZWD. We computed T_m using surface temperature measurements at Cape Grim and the coefficients of *Bevis et al.* [1992] ($T_m = 70.2 + 0.72 \times T_s$).

3. GPS Analysis

We analyzed the GPS phase observations using the GAMIT software [*King and Bock*, 1997] in 30 hour solutions (including a 3 hour overlap at the beginning and end of each UT day). The hydrostatic and wet tropospheric delays were modeled a priori by extrapolating a standard atmospheric model as a function of station height using the models of [*Saastamoinen*, 1972]. The residual zenith tropospheric delay at each site was modeled as a linear spline with knots spaced 30 min apart. The values of the delay at the knots were assumed to represent a Markov process with transition probabilities drawn from a Gaussian distribution. We limited the rate of change of the variance of the Markov process to 20 mm^2/hour and applied a long-term decorrelation time of the atmosphere of 100 hours. We mapped the delay caused by the neutral

Table 1. Baseline Lengths (in kilometers) Between Stations Used in Analysis of GPS Data

	Code	Cape Grim	Hobart	Canberra	Macquarie	Auckland
Cape Grim	GRIM	-				
Hobart	HOB2	332	-			
Tidbinbilla	TIDB	796	832	-		
Macquarie	MAC1	1 860	1 543	2 246	-	
Auckland	AUCK	2 630	2 421	2 315	2 319	-
Yaragadee	YAR1	2 931	3 211	3 197	4 391	5 373

atmosphere at any elevation to a delay in the zenith with the Niell hydrostatic and wet mapping functions [*Niell*, 1996].

We computed the ZND using GPS observations from nine different networks, encompassing different combinations of baseline lengths. Site locations used in the analysis are shown in Figure 1, distances between stations are listed in Table 1, and the sites used in each of the nine networks are shown in Table 2. We computed network 5 using elevation cutoff angles (the angle below which all observations are excluded from the analysis) between 10° and 20° in order to investigate the dependence of the PW estimates on the cutoff angle, and we also used two different mapping functions to test the sensitivity of the PW retrievals to the mapping functions. We estimated atmospheric gradients but found that this had little or no effect on the GPS estimates of PW, possibly because the gradients were of a magnitude generally less than 5 mm.

We used the precise orbits available from the IGS and did not attempt to estimate improvements to the orbits. These orbits are continuous with small (i.e., ~0.1-0.2 m) discontinuities at the day boundaries. To extend the IGS orbits beyond 24 hours we used a force model based on the BERNE model [*Beutler et al.*, 1994] to solve for 15 initial conditions of each satellite which best represented the IGS orbit. These initial conditions were then numerically integrated to create an orbit which spanned the 30 hour solutions. The average rms between our fitted orbit and the IGS orbit was ~20-30 mm.

4. MWR Analysis

A dual-frequency microwave radiometer has been in operation at Cape Grim since the beginning of November 1993 to quantify cloudiness, cloud properties, and water vapor.

Table 2. Network Configurations Used in GPS Solutions

	Network Number								
Site Name	1	2	3	4	5	6	7	8	9
Cape Grim	•	•	•	•	•	•	•	•	•
Hobart	•	•	•	•	•				
Tidbinbilla		•	•	•	•	•	•	•	•
Macquarie Island			•	•	•		•	•	•
Auckland				•	•			•	•
Yaragadee					•				•

Hill and Long [1995] and *Boers* [1996] have described the CSIRO radiometer design and the methods for obtaining liquid water and water vapor information from the measurements. The microwave system as used here can be viewed as mature technology and several good descriptions of similar systems have been published [*Hogg et al.*, 1983; *Westwater*, 1978; *Westwater et al.*, 1990]. The microwave radiometer operates at the microwave frequencies of 20.6 and 31.65 GHz where atmospheric emission depends primarily on column-integrated water vapor and liquid water present in the atmosphere. These quantities may be retrieved from continuous observations of atmospheric brightness temperatures at the two frequencies.

Atmospheric radiation is focused by a microwave reflector and a parabolic mirror onto the feedhorn of the receiver. Signals are amplified, digitized and stored on a computer. During calibration periods the detector is switched into hot (418 K) and reference (318 K) calibration sources with very stable temperatures. Nonlinearity of the detector was studied by calibrating the receiver using a microwave target immersed in liquid nitrogen and at higher temperatures using alcohol and liquid nitrogen in addition to using the reference and hot sources. The response of the receiver is linear from 418 K down to 77 K. The extrapolation to the brightness temperature range observed in the atmosphere (10 K to 40 K) is also expected to be linear because nonlinearity of the detector is most likely to manifest itself at high rather than low radiances.

In order to retrieve PW, calibration and retrieval constants are required. The calibration constants relate the receiver output voltage to brightness temperature, while the retrieval constants relate brightness temperature to PW. The calibration constants were determined using radiosonde temperature and humidity observations taken during noncloudy conditions (33 of the 116 profiles during ACE1). Brightness temperatures were calculated for clear-sky conditions using a layered model of the atmosphere and absorption coefficients for water vapor and oxygen presented by *Chiswell et al.* [1994]. The calibration coefficients are chosen to optimize, in a least squares sense, the fit between the modeled and the observed brightness temperatures.

Calibration constants can also be determined by performing tipping curve scans whereby the receiver is scanned toward the horizon so that increasingly larger air masses are observed. When the opacity in each channel is plotted versus air mass, the resulting line should pass through the origin. The offsets of the lines from the origin yields estimates of the calibration constants. Several sets of tipping curve scans were performed during ACE1 and the brightness temperatures calculated were very close to those obtained using the radiosonde calibration procedure; thus our choice of using the former rather than the latter was arbitrary.

Our receiver model to convert the system voltages to brightness temperatures omits specific losses due to the reflector and parabolic mirror. The parabolic mirror is located inside the radiometer housing, and its temperature variations are small because the whole instrument is located inside an air-conditioned and insulated shipping container. A general mean loss factor associated with these surfaces is incorporated during calibration; however, it is conceivable that variations in the external temperature still affect the interior temperature. We investigated this potential problem by comparing the deviations between GPS and MWR water vapor output (shown below) with the outside temperature and time of day (i.e., whether the reflector was in sunlight or shade). It was found that most of the differences between the GPS and the MWR were at night, or at times when there were thick clouds. Therefore we do not believe that high-temperature perturbations influence the accuracy of our calibration coefficients.

The optical depths τ_1 and τ_2 of the atmosphere at the frequencies of the radiometer channels are deduced from the corresponding brightness temperatures T_1 and T_2 via

$$\tau_i = \ln\left(\frac{T_{mr} - T_{bg}}{T_{mr} - T_i}\right) \tag{4}$$

[*Davis*, 1986; *Rocken* ,1988], where T_{bg} is the contribution from background sources and T_{mr} is the mean radiating temperature. The latter was fixed at the climatological value for Cape Grim, deduced from analysis of 8 years of radiosonde ascents at Hobart and Laverton, the nearest radiosonde stations in the radiosonde archive maintained by the Australian Bureau of Meteorology. Hobart is approximately 300 km to the south of Cape Grim, while Laverton is approximately 300 km to the north. Although *Chiswell et al.* [1994] show that the use of a

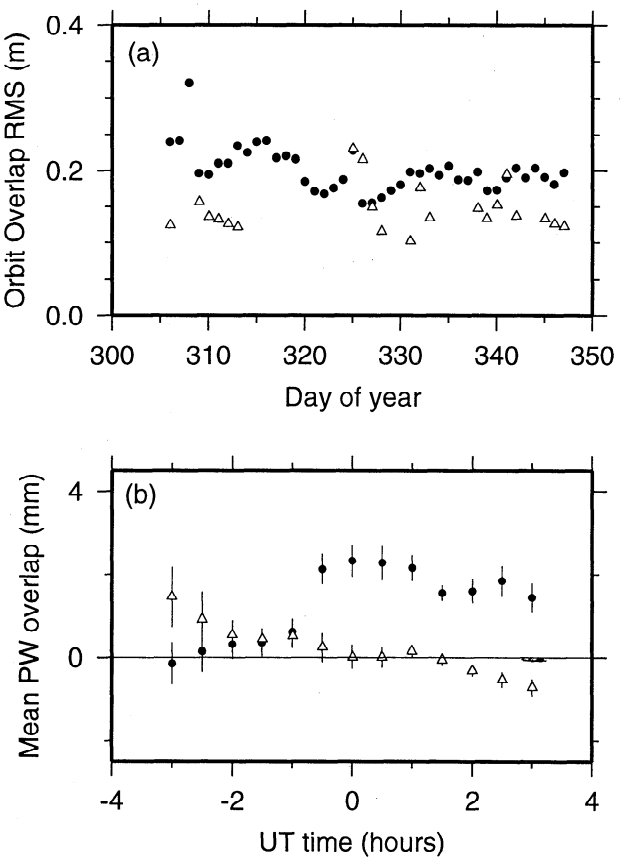

Figure 2. Root mean square (rms) of 3 hour overlaps of orbits and 6 hour average overlaps of precipitable water vapor (PW) estimates: (a) rms of orbit overlaps using International GPS Service (IGS) orbits (circles) and our estimated orbits (triangles); (b) rms of PW estimates using IGS orbits (circles) and our estimated orbits (triangles). Each point in Figure 2b represents a mean of estimates of the parameter at the relevant time from all the days which were analyzed. One sigma uncertainties of single estimates are plotted.

climatological estimate for T_{mr} can cause significant biases in PW at continental sites, we found that the annual range of T_{mr} was small in the maritime environment of Cape Grim.

The water vapor path PW is linearly linked to the optical depths by

$$\mathrm{PW} = B_0 + B_1\tau_1 + B_2\tau_2 \quad (5)$$

where B_1 and B_2, the retrieval coefficients, are determined by regressing the measured brightness temperatures against precipitable water. Three data sets were used for the regression, the first containing 131 radiosondes launched at Cape Grim during ACE1, the second containing the climatology of approximately 5600 ascents at Hobart referred to above, and the last being a similar climatology at Laverton. The retrieval coefficients derived with Cape Grim ascents were closer to those with Hobart ascents, but in principle, both sets could be used to invert brightness temperatures to water vapor. *Robinson* [1988], *Sheppard et al.* [1991], and *Sheppard* [1996] have questioned the validity of the linear model as expressed in (4); however, it can be shown that for the maritime climate of Cape Grim with moderate seasonal changes in atmospheric temperature and a limited range of PW (generally between 10 and 30 mm), the linear model suffices.

5. Sensitivity Analysis

5.1. Accuracy of GPS Satellite Orbits

The discontinuities of the IGS orbits at the day boundaries led to discontinuities in the PW time series of up to 2 mm. Figure 2a shows the mean rms of a 3 hour overlap of the IGS orbits, while Figure 2b shows the mean PW overlap error at half hourly intervals during the 6 hour overlapping period of neighboring days. There is clearly a bias in the PW overlaps which changes as a function of time, reaching a maximum of about 2 mm at about 0000 UT. We reduced the orbit overlap errors by computing global orbits using data from about 60 IGS stations and constraining the coordinates of 47 of these stations to their ITRF96 values [*Altamimi*, 1998]. The resulting orbit overlap errors are significantly reduced (Figure 2a) and the corresponding PW overlaps show no significant bias up to 1 hour either side of 0000 UT (Figure 2b). We concluded that the day boundary overlap biases seen in the PW estimates were related to discontinuities in the IGS orbits and found that our estimated satellite orbits were more accurate. The improvement in orbit accuracy is due to a more accurate definition of the terrestrial reference frame; overlap errors for IGS orbits in 1998 are typically ~13 cm rms, the same level as our computed orbits for the 1995 data. We used our estimates of the satellite orbits to compute all the solutions discussed in this paper.

5.2. A Priori Coordinates and Constraints

The GPS estimates of PW are sensitive to the number of constraints applied to the site coordinates in the network. In a comparison of GPS and MWR PW estimates, both the magnitude of the bias and the sigma of a single observation vary according to the number of a priori constraints imposed on the site coordinates, with the optimal approach being tight constraints applied to at least the three dimensional coordinates of TIDB and YAR1 and the height of GRIM (Figure 3). We chose the level of a priori constraint to be the ITRF94 uncertainty for the coordinates of TIDB and YAR1 (~± 2mm), although the same results are generated if these coordinates are fixed rather than tightly constrained. We estimated the height of GRIM from an average of all daily estimates from solutions with the height of GRIM loosely constrained. Applying additional constraints to the coordinates of other sites does not improve the GPS-MWR PW comparison. We introduced a 50 mm height error at TIDB (while constraining the height of GRIM) which in turn biased the GPS PW estimates by about -0.5 mm, indicating that it is essential that the heights are constrained at the correct values. Similarly, it is critical that the offsets of the electrical phase centers of each antenna are correctly applied. All antennas in this experiment were Dorne Margolin *T* or *B* type antennas, and we used the phase center offset values in the IGS table IGS_01 (available from the IGS Central Bureau Information System [*Gurtner et al.*, 1995]). The most recent antenna phase center models use the same offset from the preamp base to the phase centers as the models of *Gurtner et al.* [1995]. Since all the more recent models are relative to Dorne Margolin antennas (i.e., there are no elevation corrections in these models for the Dorne Margolin antennas), we could not apply any elevation angle dependent corrections to the phase centers.

5.3. Elevation Cutoff Angle

We analyzed all the data using network 5 and varied the elevation cutoff angle between 10° and 20° in 1° increments. While other GPS analyses are now performed using cutoff angles of less than 10° [e.g., *Rothacher et al.*, 1997], we were limited to a minimum of 10° because the wooden fence

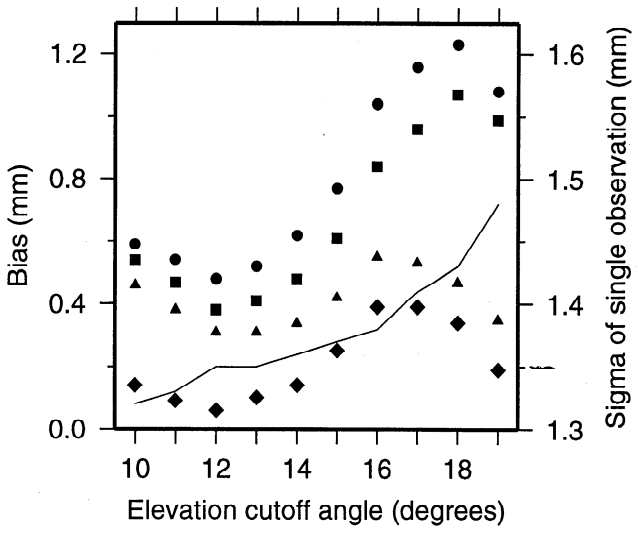

Figure 3. Bias of comparison of GPS and microwave radiometer (MWR) estimates of PW using the Niell wet mapping function for elevation cutoff angles of 10° to 19° with different numbers of coordinate constraints in the GPS solutions: TIDB (circles); TIDB and YAR1 (squares); TIDB, YAR1, and the height of GRIM (triangles). Solutions using the CFA2.2 wet mapping function and constraints on the coordinates of TIDB, YAR1, and the height of GRIM are shown as diamonds. The (one sigma) standard deviation of a single observation is shown as a solid line and is not significantly affected by different numbers of coordinate constraints.

surrounding the antenna at Tidbinbilla obscured the horizon below 10° (R. Jenkins, Tidbinbilla Tracking Station, personal communication, 1997). The scatter of the GPS PW with respect to the MWR PW increases as the elevation cutoff angle is increased and a systematic bias is introduced in the comparison of the GPS and MWR estimates (Figure 3). This indicates that there is a loss of sensitivity to the ZWD when only high-elevation ray paths are used in the GPS analyses, suggesting that the most accurate estimates of PW from GPS observations will be obtained using a low-elevation cutoff angle.

A cutoff angle of 12° seems to result in the smallest bias between the two systems. Why are the estimates using observations below 12° less accurate? When low angle elevation data are included in the analysis, small changes in PW within the model will cause large variations in the delay along the low-elevation paths, so the sensitivity of the retrieval process is increased. However, the gain in sensitivity must be balanced against the increasing uncertainty of the mapping function for very low elevation angles along with the increased noise of the GPS observations due to effects such as multipath and antenna phase center variations. For this data set, utilizing low-angle observations has the effect of introducing a bias into the GPS/MWR comparisons which increases as a function of the level of PW present, with the GPS estimate being lower than the MWR estimate. Hence the computation of a mean bias is affected by this nonlinearity which results in the 12° solution appearing to be the optimal solution. We chose 12° as being the compromise elevation cutoff angle for this experiment.

5.4. Mapping Functions

We analyzed the GPS data using both the CFA2.2 mapping function of *Davis et al.* [1985] (the same function is used for both hydrostatic and wet delays) and the Niell hydrostatic and wet mapping functions and found that the Niell mapping functions introduced a significant decrease in the GPS PW estimates. The CFA and Niell (hydrostatic) mapping functions are effectively the same down to 10° but the Niell (wet) and the CFA mapping functions differ by up to 7 mm mapped delay at 10°. The difference is less than 0.07%; however, this changes the PW estimates by up to 0.7 mm (Figure 4). Thus the estimation of PW is sensitive to small changes in the mapping functions. We found that the bias between the GPS and the MWR estimates was significantly smaller when using the CFA wet mapping function rather than the Niell wet mapping function (Figure 3), while the standard deviation of a single observation was not affected. This indicates that there is high sensitivity of the PW estimates to small changes in the wet mapping function and suggests that the marine-influenced atmospheric environment of Cape Grim may not be well modeled by a mapping function derived from ray tracing elsewhere. *Davis et al.* [1985] derived the CFA2.2 model from ray traces through a theoretical atmosphere and expected their model to be applicable to 5°, while *Niell* [1996] derived mapping functions from seasonal atmospheric data in North America and claimed that they are accurate to 3°.

One could create a mapping function specific to Cape Grim by ray tracing through atmospheres with temperature and water vapor profiles estimated from the 116 radiosonde launches during the ACE1 experiment to generate a mapping function which is specifically tailored to the site of interest. However, this is not a practical approach, which is readily applicable to many GPS sites owing to the need for data from radiosonde launches. While such a mapping function would probably be valid only for Cape Grim and the nearby region, it may indicate that better results are obtained if the wet mapping function is tailored to the specific site of interest rather than relying on a global model.

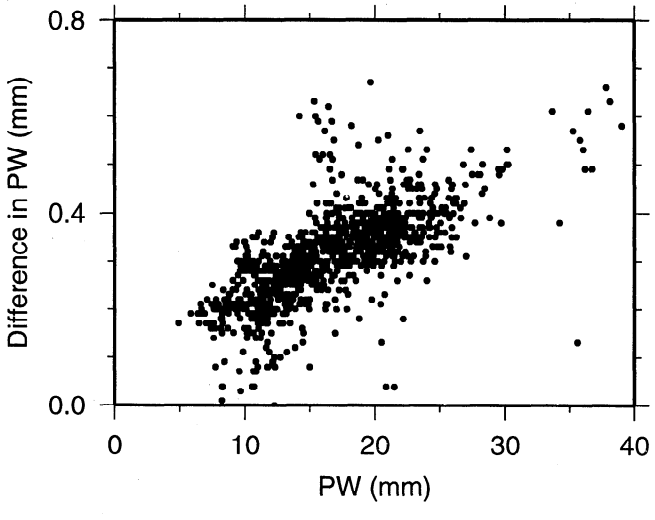

Figure 4. Differences in estimates of PW using Niell and CFA2.2 wet mapping functions versus the magnitude of PW.

5.5. Network Configuration

The magnitude of the bias and the scatter about the mean of the comparison of GPS and both radiosonde and MWR estimates of PW are clearly related to the lengths of the baselines in the GPS solutions (Table 3). *Duan et al.* [1996] found agreement of ~1.2 to 1.5 mm between MWR and GPS estimates of PW, and it is not until the inclusion of a baseline of more than 2000 km that we achieve this level of agreement. The inclusions of the 700 km baseline (GRIM to TIDB) and 1800 km baseline (GRIM to MAC1) do not provide sufficient decorrelation of the elevation angles to the satellites from the two sites in close proximity (GRIM and HOB2 with a separation of less than 350 km) to enable estimation of the PW with a precision better than 1.5 mm. This result is in contrast with the simulations of *Rocken et al.* [1993] who claimed that the minimum required length of baselines was 500 km in order to accurately estimate absolute PW values. They also claimed that with perfectly known orbits and hydrostatic delay and baselines of up to 1000 km, it was not possible to estimate absolute PW to better than 1.5 mm rms. Our results support this claim, but we show that with even longer baselines one can achieve an even higher level of accuracy.

There is little change in the agreement of GPS and MWR estimates between networks 4 and 5, indicating that a single distant site is sufficient in order to achieve accurate absolute estimates of PW from GPS observations (Table 3). However, the bias between GPS and radiosonde estimates is reduced with the addition of YAR1 to the GPS network. Comparisons of networks 4 with 8 and 5 with 9, where the only differences are that the nearby site of HOB2 has been omitted, show that the inclusion of a near site has no effect on the precision of the estimates of PW at GRIM. Thus it is feasible to install a single GPS station and estimate the absolute levels of PW accurately

Table 3. Comparisons of GPS, MWR, and Radiosonde PW Estimates for Different Network Configurations

	MWR-GPS		Radiosonde-GPS	
Network	Bias, mm	Sigma, mm	Bias, mm	Sigma, mm
1	0.46	2.4	0.3	2.7
2	0.37	1.6	0.5	2.1
3	0.49	1.4	0.3	1.6
4	0.07	1.4	0.7	1.6
5	0.05	1.3	0.6	1.5
6	-0.10	2.0	1.2	2.4
7	0.25	1.4	0.6	1.6
8	-0.10	1.4	1.0	1.6
9	0.00	1.3	0.7	1.5

The bias represents the mean offset between the estimates of the systems, and the (one sigma) standard deviation a single observation is computed about the mean offset.

by analyzing the local data with the surrounding IGS tracking stations.

6. Results

The closest agreement between GPS and MWR estimates of PW was obtained using a 12° elevation cutoff angle, a six station network with the three-dimensional coordinates of TIDB and YAR1 and the height of GRIM constrained to ±2 mm, the Niell hydrostatic mapping function, and the CFA2.2 wet mapping function. Comparisons of the three techniques are shown in Figure 5 and a bias (or mean difference) between PW estimated from the GPS, MWR, and radiosonde techniques, and a (one sigma) standard deviation of a single observation are shown in Table 3 (the MWR estimates of PW were averaged over 30 min intervals for comparison with the GPS estimates). The MWR estimates agree with the radiosonde estimates to ±1.5 mm with a bias of 0.7 mm, although there is a tendency for the MWR to overestimate the level of PW for values higher than 20 mm (see Figure 5 and discussion below), while the agreement between estimates from GPS and radiosonde is about ±1.5 mm with a bias of 0.6 mm.

Figure 6 shows a comparison of PW estimated by GPS, MWR, and radiosonde launches for days of year 326-348. We include this figure to demonstrate that the results in this paper show, in a general sense, the same level of high correlation between all three observing techniques as reported elsewhere; however, in the following section we will analyze some particular circumstances which demonstrate that the difference between GPS and MWR on certain occasions can be as large as 3-4 mm PW.

7. Discussion

7.1. Microwave Radiometer Overestimation

There is a tendency for the microwave PW values to be higher than the GPS PW values for PW > 25 mm. Similarly, the MWR PW values are higher than the radiosonde PW values in the same region (Figures 7 and 5c), suggesting that the MWR PW may be overestimated by several millimeters for PW > 25 mm. We have investigated several potential causes of this overestimation. Errors in the traditional processing techniques which include models of the waveguide losses associated with converting the radiometer voltages to brightness temperatures can probably be ruled out because such models are essentially linear, while plots such as Figure 5 suggest a nonlinearity. There are four possible sources for nonlinearity that could explain an overestimate of MWR PW as seems to be present in Figure 5.

The first one is that the mean atmospheric radiating temperature, assumed to be constant in the retrieval, is varying with PW. This problem was investigated by *Chiswell et al.*

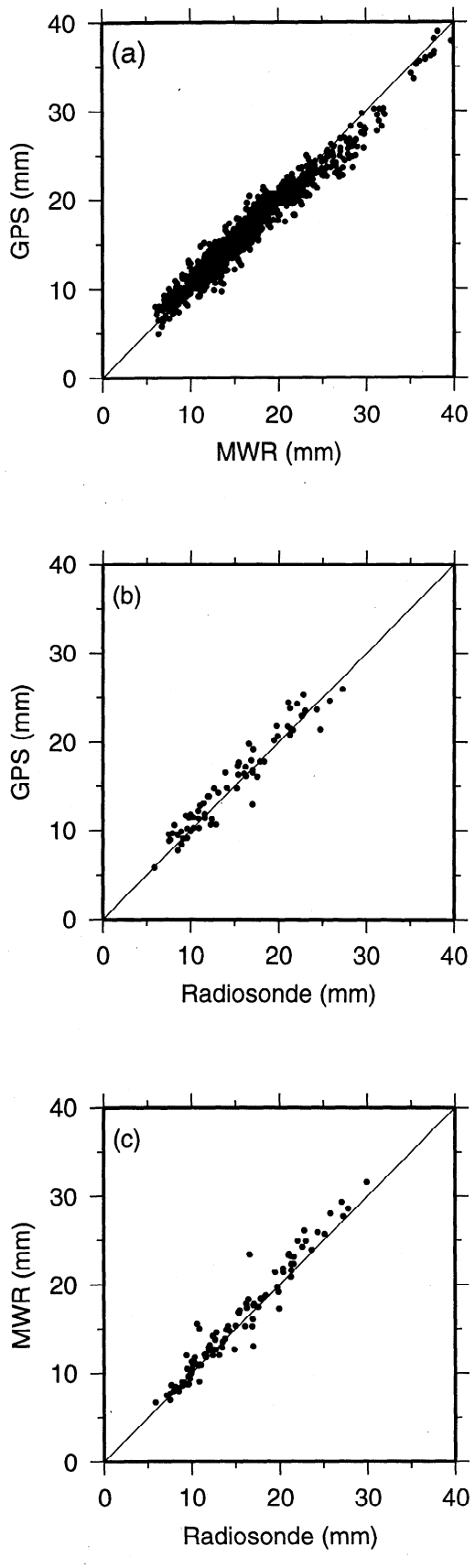

Figure 5. Comparisons of estimates of PW for network 5 using an elevation cutoff angle of 12°: (a) GPS and MWR, (b) GPS and radiosonde, (c) MWR and radiosonde.

[1994] for a continental U.S. site where the temperature could vary seasonally by up to 30 K. Using the set of 5600 radiosonde profiles taken at Hobart, it can be shown that the mean atmospheric radiating temperature is weakly varying with the water vapor path. Using the model $T_{mean} = a + b \times PW$, we performed an adaptive retrieval by computing PW using the routine linear retrieval algorithm, then updating T_{mean} and recomputing PW. Convergence to one value of PW is very rapid and the adaptive technique demonstrates that a small percentage of points benefits from using this model; however, the computed differences of 1 mm with the original retrieval procedures are too small to account for the 4 mm differences between the GPS and the MWR estimates.

The second possibility is the presence of raindrops, investigated by *Shepard* [1996] and *Shepard et al.* [1991]. The presence of raindrops invalidates the assumption of pure absorption in the radiative transfer equation that forms the basis of most microwave retrieval algorithms. However, scattering at frequencies below 90 GHz is at least 3 orders of magnitude smaller than absorption by liquid water droplets smaller than 100 μm diameter. Since periods of precipitation detected at the surface were omitted from the data prior to any comparison with the GPS data, the only possibility for this type of error being introduced into the analysis is through such precipitation droplets evaporating below the cloud base before reaching the ground. This effect is difficult to estimate although we suspect it to be minimal due to the overall high-moisture content of the subcloud boundary layer. Rain also invalidates the linear model of equation (4). We investigated the effect of clouds on the GPS - MWR comparisons by omitting all data for which the 30 GHz channel showed the presence of liquid water. This reduced the number of data points considerably but essentially preserved the shape of Figure 5, which rules out the presence of clouds or rain as a possible source for the nonlinearity.

The third possibility is instability of the receiver waveguide temperature which is an essential parameter in the microwave calibration procedure. On several occasions we found that the waveguide temperature experienced diurnal fluctuations of up to 2° C which appeared to be related to the inability of the air conditioning unit to control the temperature under hot conditions. However, none of these periods coincided with periods where the MWR exceeded the GPS PW values, so this problem can also be dismissed.

The fourth possibility is a nonlinearity of the receiver hardware. As mentioned earlier, we believe that this problem can be eliminated on account of our receiver calibration using a cryogenic target. Although it is difficult to ascertain whether linearity extends from 77 K down to the brightness temperatures measured in the atmosphere, we expect this problem to be minimal.

8. Conclusions

GPS can be used to estimate absolute levels of PW with an accuracy of ±1.3 mm. The GPS PW estimates are sensitive to the network configuration used in the analysis of the GPS phase data, and solutions which do not include baselines longer than 2000 km have a larger bias and a higher scatter with respect to the radiosonde and MWR estimates. The requirement for baselines greater than 2000 km is in contrast with the conclusions of *Rocken et al.* [1993] who claimed from simulated data that a separation of more than 500 km was

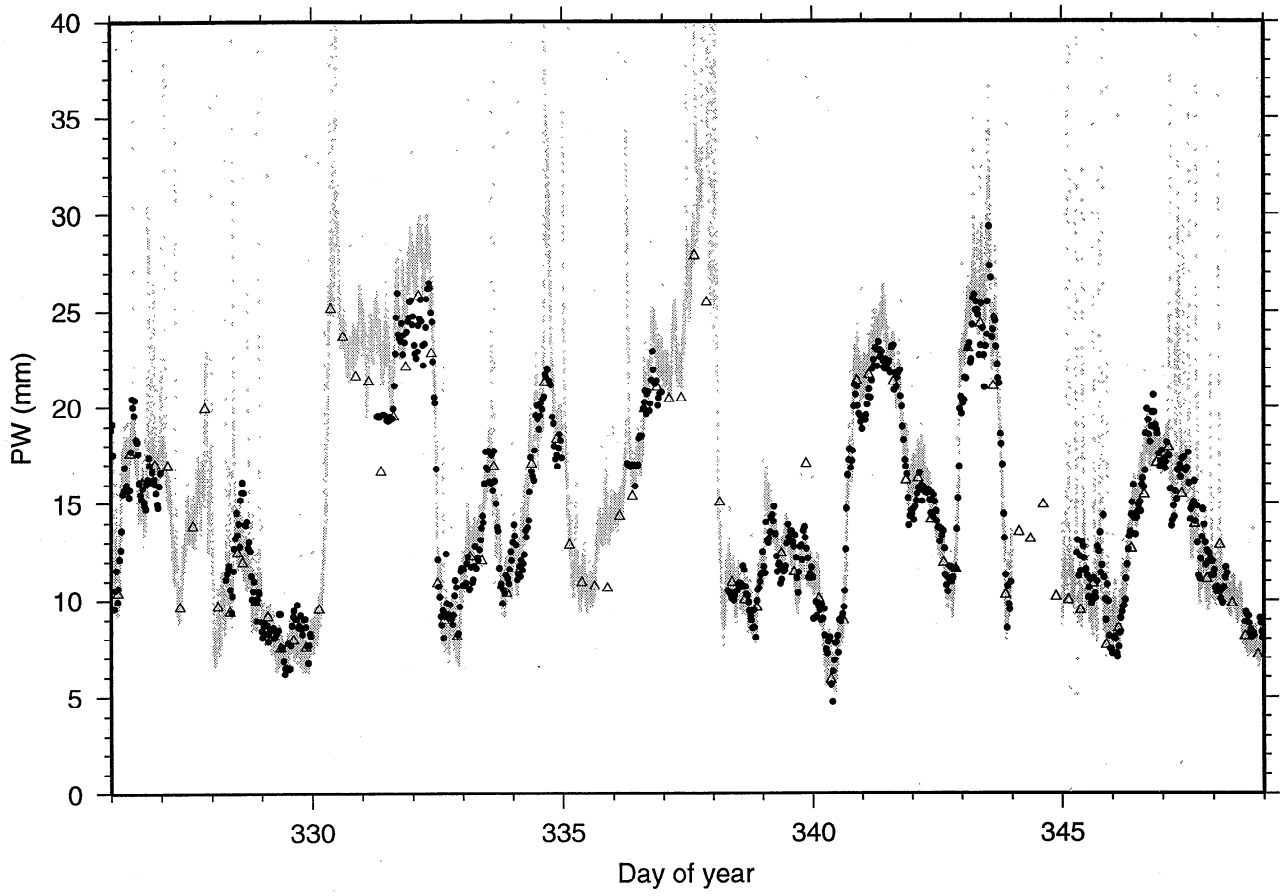

Figure 6. Time series of estimates of PW from GPS (solid circles), MWR (grey circles), and radiosonde (open triangles) for the period where radiosonde data were available (days of year 326-348). GPS data for days 330, 335, and 337 were not collected due to receiver malfunctions at GRIM, while AUCK data were missing on day 344. The large spikes evident in the MWR PW (eg on days 334, 337, 345-348) are due to rain and were removed from the final comparisons between the GPS and the MWR data.

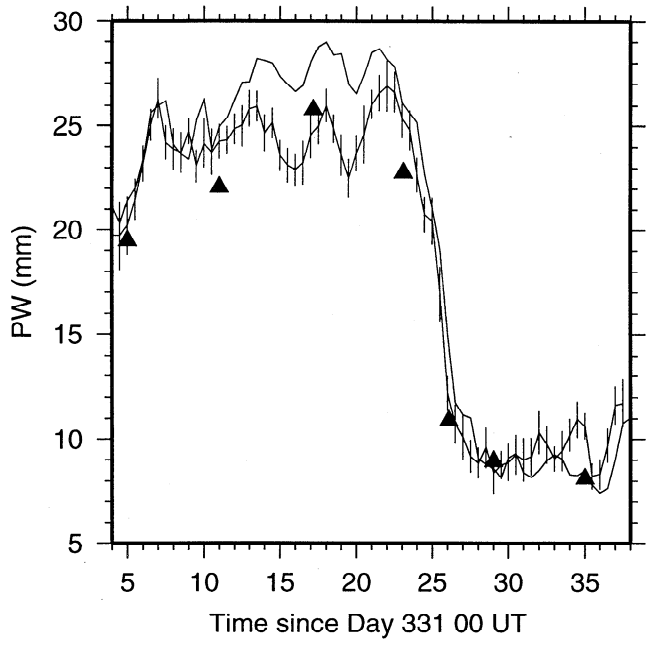

Figure 7. Comparison of GPS (with error bars), MWR (solid line), and radiosonde data (triangles) for days of year 331 and 332.

sufficient for absolute estimation of PW. The Niell wet mapping function was found to introduce a bias of about -0.3 mm in the PW estimates, and we found closer agreement when using the CFA2.2 mapping function for mapping the wet delay from the zenith to any elevation angle. The rms and the bias of the GPS PW retrieval increases with increasing elevation cutoff angle and we showed that an elevation cutoff angle of 12° produced the closest agreement between the GPS and the MWR estimates.

We found that discontinuities of about 20 cm rms in the IGS orbits at the day boundaries introduced discontinuities of about 2 mm in overlapping estimates of PW. The effects of orbital errors on PW estimates were reduced to insignificant levels by recomputing the GPS orbits using a 60 station tracking network and constraining the coordinates of the 47 core IGS sites to their ITRF96 values. The overlap error of the recomputed orbits was typically ~12-15 cm and resulted in an average bias of 0.0 mm PW at the day boundary.

For values of PW larger than 25 mm we found that occasionally the GPS analysis underestimated and the MWR system overestimated the level of PW compared to the estimate from radiosonde launches. The causes of these differences are unclear but may be related to errors in the mapping functions due to localized irregularities in the atmospheric profile above Cape Grim and/or aspects of the microwave radiometer receiver hardware that are presently not understood.

Acknowledgments. The radiosonde profiles collected at Cape Grim during the ACE1 were obtained using the Integrated Sounding System (ISS) operated by personnel from the National Center for Atmospheric Research (NCAR) in Boulder, Colorado. We thank Mike Bevis and Bob King for fruitful discussions on the GPS analysis. The staff at the Cape Grim Baseline Air Pollution Station and the mechanical and electronics workshops at CSIRO Division of Atmospheric Research are acknowledged for keeping the systems running at all times, sometimes under testing weather conditions. We acknowledge the comments of two anonymous reviewers, which improved the manuscript.

References

Altamimi, Z., IGS reference stations classification based on ITRF96 residual analysis, paper presented at the IGS Workshop, Int. GPS Serv. for Geodyn., Darmstadt, Germany, Feb. 9-11, 1998.

Askne, J., and H. Nordius, Estimation of tropospheric delay for microwaves from surface weather data, *Radio Sci., 22*, 379-386, 1987.

Bates, T. S., B. J. Huebert, J. L. Gras, F. B. Griffiths, and P. A. Durkee, The International Global Atmospheric Chemistry (IGAC) project's first Aerosol Characterization Experiment (ACE1): Overview, *J. Geophys. Res.*, in press, 1997.

Beutler, G., E. Brockmann, W. Gurtner, U. Hugentobler, L. Mervart, M. Rothacher, and A. Verdun, Extended orbit modeling techniques at the CODE processing center of the International GPS Service for Geodynamics (IGS): Theory and initial results, *Manuscr. Geod., 19*, 367-386, 1994.

Bevis, M., S. Businger, T. A. Herring, C. Rocken, R. Anthes, and R. H. Ware, GPS meteorology: Remote sensing of atmospheric water vapor using the global positioning system, *J. Geophys. Res., 97*, 15,787-15,801, 1992.

Bevis, M., S. Businger, S. Chiswell, T. A. Herring, R. A. Anthes, C. Rocken, and R. H. Ware, GPS meteorology: Mapping zenith wet delays onto precipitable water, *J. Appl. Meteorol., 33*, 379-386, 1994.

Boers, R., Microwave observations of liquid water path and water vapor path at Cape Grim, *Baseline, 1994-1995*, 22-29, 1996.

Chiswell, S. R., S. Businger, M. Bevis, F. Solheim, C. Rocken, and R. Ware, Improved retrieval of integrated water vapor from water vapor radiometer measurements using numerical weather prediction models, *J. Atmos. Oceanic Technol., 11*, 1253-1261, 1994.

Davis, J. L., Atmospheric propagation effects on radio interferometry, *Sci. Rep. 1, AFGL-TR-86-0243*, 276 pp., Air Force Geophys. Lab., Bedford, Mass., 1986.

Davis, J. L., T. A. Herring, I. I. Shapiro, A. E. E. Rogers, and G. Elgered, Geodesy by radio interferometry: Effects of atmospheric modeling errors on estimates of baseline length, *Radio Sci., 20*, 1593-1607, 1985.

Duan, J., M. et al., GPS meteorology: Direct estimation of the absolute value of precipitable water, *J. Appl. Meteorol., 35*, 830-838, 1996.

Elgered, G., J. L. Davis, T. A. Herring, and I. I. Shapiro, Geodesy by radio interferometry: Water vapor radiometry for estimation of the wet delay, *J. Geophys. Res., 96*, 6541-6555, 1991.

Emardson, T. R., G. Elgered, and J. M. Johansson, Three months of continuous monitoring of atmospheric water vapor with a network of Global Positioning System receivers, *J. Geophys. Res., 103*, 1807-1820, 1998.

Gu, M., and F. K. Brunner, Theory of the two frequency dispersive range correction, *Manuscr. Geod., 15*, 357-361, 1990.

Gurtner, W., and R. Lui, The Central Bureau Information System, in *International GPS Service for Geodynamics, Ann. Rep. 1994*, edited by J. Z. Zumberge, R. Lui, and R. Nielan, Jet Propul. Lab., Calif., 1995.

Herring, T. A., Modeling atmospheric delays in the analysis of space geodetic data, in *Symposium on Refraction of Transatmospheric Signals in Geodesy*, Publ. Geod., edited by J. C. De Munk and T. A. Spoelstra, pp. 157-164, Netherlands Geodetic Commission, Delft, Netherlands, 1992.

Hill, R. H., and A. B. Long, The CSIRO dual-frequency microwave radiometer, *Tech. Pap., 35*, CSIRO Div. of Atmos. Res., Melboune, 1995.

Hogg, D. C., F. O. Guiraud, J. B. Snider, M. T. Decker, and E. R. Westwater, A steerable dual-channel microwave radiometer for measurements of water vapor and liquid in the troposphere, *J. Clim. Appl. Meteorol., 22*, 789 - 806, 1983.

King, R. W., and Y. Bock, Documentation for the GAMIT GPS analysis software, release 9.66, Mass. Inst. of Technol., Cambridge Mass., 1997.

MacMillan, D. S., and C. Ma, Evaluation of very long baseline interferometry atmospheric modeling improvements, *J. Geophys. Res., 99*, 637-651, 1994.

Neilan, R.E., IGS organization and the international tracking network, in *International GPS Service for Geodynamics, Ann. Rep. 1996*, edited by J. Z. Zumberge, D.E. Fulton, and R.E. Nielan, Jet Propul. Lab., Calif., 1997.

Niell, A.E., Global mapping functions for the atmospheric delay at radio wavelengths, *J. Geophys. Res., 101*, 3227-3246, 1996.

Quinn, K. J., and T. A. Herring, GPS Atmospheric water vapor measurements without surface pressure sensors, *Eos Trans. AGU, Fall Meet. Suppl.*, 77 (46), 134, 1996.

Robinson, S. E., The profile algorithm for microwave delay estimation from water vapor radiometer data, *Radio Sci., 23*, 401-408, 1988.

Rocken, C., The Global Positioning System: A new tool for tectonic studies, 298 pp, Ph.D. thesis, Univ. of Colo, Boulder, 1988.

Rocken, C., R. Ware, T. van Hove, F. Solheim, C. Alber, J. Johnson, M. Bevis, and S. Businger, Sensing atmospheric water vapor with the global positioning system, *Geophys. Res. Lett, 20*, 2631-2634, 1993.

Rocken, C., T. van Hove, J. Johnson, F. Solheim, R. Ware, M. Bevis, S. Chiswell, and S. Businger, GPS/STORM - GPS sensing of atmospheric water vapor for meteorology, *J. Atmos. Oceanic Technol., 12*, 468-478, 1995.

Rothacher, M., T. A. Springer, S. Schaer, and G. Beutler, Processing strategies for regional GPS networks, in *Proceedings of IAG General Assembly*, Int. Assoc. of Geod., Rio de Janeiro, Brazil, Sept. 3-9, 1997.

Saastamoinen, J., Atmospheric correction for the troposphere and stratosphere in radio ranging of satellites, in *The Use of Artificial Satellites for Geodesy, Geophys. Monogr. Ser.*, vol. 15, edited by S. W. Henriksen, A. Mancini, and B. H. Chovitz, pp. 247-251, AGU, Washington, D. C., 1972.

Sheppard, B. E., Effect of rain on ground-based microwave radiometric measurements in the 20 - 90 GHz range, *J. Atmos. Oceanic Technol., 13*, 1139-1151, 1996.

Sheppard, B. E., R. E. Steward, and G. A. Isaac, Non-linear optimal estimation of temperature and integrated water vapor and liquid using a ground-based microwave radiometer in coastal winter storms, *J. Atmos. Oceanic Technol., 8*, 812-825, 1991.

Smith, E. K., and S. Weintraub, The constants in the equations for atmospheric refractive index at radio frequencies, *J. Res. Natl. Bur. Stand., 50*, 39-41, 1953.

Spilker, J. J., Jr., GPS signal structure and performance characteristics, *J. Inst. of Nav.*, Global Positioning System special issue, pp. 29-54, 1980.

Westwater, E. R., The accuracy of water vapor and cloud liquid water determination by dual frequency ground-based microwave radiometry, *Radio Sci., 13*, 677 - 685, 1978.

Westwater, E. R., J. B. Snider, and M. J. Falls, Ground based radiometric observations of atmospheric emission and attenuation at 20.6, 31.65 and 90.0 GHz: A comparison of measurements and theory, *IEEE Trans. Antennas Propag., 38*, 1569 - 1580, 1990.

R. Boers and D. M. O'Brien, CSIRO Atmospheric Research, Aspendale, VIC 3195, Australia. (e-mail: reb@dar.csiro.au, dob@dar.csiro.au)

M. Hendy, Australian Surveying and Land Information Group, Fern Hill Park, Bruce, A.C.T. 2601, Australia. (e-mail: martin.hendy@auslig.gov.au)

P. Tregoning, Research School of Earth Sciences, The Australian National University, Canberra, A.C.T. 0200, Australia. (e-mail: pault@rses.anu.edu.au)

(Received January 26, 1998; revised April 24, 1998;
accepted July 27, 1998.)